Journal of The Electrochemical Society, **154** (10) J310-J313 (2007)
0013-4651/2007/154(10)/J310/4/$20.00 © The Electrochemical Society

Host Sensitized White Luminescence from $ZnGa_2O_4:Dy^{3+}$ Phosphor

K. Mini Krishna, G. Anoop,* and M. K. Jayaraj**

Optoelectronic Devices Laboratory, Department of Physics, Cochin University of Science and Technology, Kochi 682 022, India

Dysprosium-doped zinc gallate phosphors with the nominal formulas $ZnGa_{2(1-x)}O_4:Dy_{2x}$ were prepared by the high-temperature conventional solid-state reaction technique, the dopant concentration being varied in the range $0 \leq x \leq 0.025$. $Zn_{1-x}Ga_2O_4:Dy_x$ and $Ga_{2(1-x)}O_3:Dy_{2x}$ samples were also prepared for comparison for a dopant concentration of $x = 0.02$. Only the intrinsic self-activated emission of the $ZnGa_2O_4$ host is observed in the photoluminescence emission spectra of $Zn_{0.98}Ga_2O_4:Dy_{0.02}$, while both the host emission band and characteristic emission lines ($^4F_{9/2} \rightarrow {}^6H_J$) of Dy^{3+} are observed for $ZnGa_{2(1-x)}O_4:Dy_{2x}$ and $Ga_{1.98}O_3:Dy_{0.04}$ phosphors. The luminescent intensity differs in the phosphors due to the different energy-transfer rates from the respective hosts to the luminescent centers. Photoluminescent studies reveal the fact that Dy^{3+} ions replace Ga^{3+} ions in the host lattice at their octahedral sites. The source of white luminescence in the doped samples is the nonradiative resonant energy transfer via exchange interaction between the host and the activator. The CIE coordinates of the 2.5 atom % Dy^{3+}-doped sample (0.32, 0.33) matches well with achromatic white (0.33, 0.33) on the chromaticity diagram.
 [DOI: 10.1149/1.2766607]

Manuscript submitted March 2, 2007; revised manuscript received June 4, 2007. Available electronically August 10, 2007.

A major challenge in the area of flat panel display (FPD) technology is the identification of new multicolor or white-light-emitting phosphor materials for application in electroluminescent displays (ELDs), plasma display panels (PDPs), and field emission displays (FEDs). A suitable blend of currently available efficient blue, green, and red phosphors and light-emitting diodes (LEDs) gives a natural remedy to this issue.[1,2] Co-doping in a single host lattice also gives desirable results[3,4] with better luminous efficiency than the former. But a more feasible approach is via the combination of multicolor emissions from a single luminescence center. Rare-earth (RE) ions serve as excellent activators in modern lighting and display fields due to their characteristic emissions from 4f-4f or 5d-4f transitions. But the phosphor hosts activated with RE ions should possess a strong and broad absorption band in the UV or vacuum UV (VUV) region of the electromagnetic spectrum for efficient and effective excitation. This is because RE ions strongly absorb in the short wavelength of the UV region and weakly absorb in the near-UV to blue spectral region.

Trivalent dysprosium, a RE with $4f^9$ electronic configuration, is known to emit two intense fluorescence transitions, $^4F_{9/2} \rightarrow {}^6H_{15/2}$ in the blue and $^4F_{9/2} \rightarrow {}^6H_{13/2}$ in the yellow-orange wavelength region.[5,6] The latter, being a hypersensitive transition ($\Delta L = 2$, $\Delta J = 2$), is strongly influenced by the crystal-field environment. At a suitable yellow-to-blue intensity ratio, Dy^{3+} emits white light.[7,8] Unlike the RE dopants Eu^{3+} and Tb^{3+}, the luminescence of Dy^{3+} cannot be excited using the common fluorescent lamps that have a strong and broad absorption band around 254 nm. This is because the charge-transfer absorption band (CTB) and $4f^9$-$4f^8$5d excitation band of Dy^{3+} are located below 200 nm. This drawback of Dy^{3+} luminescence can be overcome either by host sensitization[9,10] or by impurity ion sensitization.[11]

Oxide phosphors serve as a potential host over sulfide phosphors due to their superior stability, both chemical and thermal, against electron bombardment and excellent luminescent properties. Zinc gallium oxide is one among the oxide phosphors that has attracted much attention since the last decade as a promising phosphor for use in thin-film ELDs[12-14] and for low-voltage applications in FEDs[15] and vacuum fluorescent displays (VFDs).[16] It has *Fd3m* space group symmetry and crystallizes in the normal spinel structure with Zn^{2+} ions occupying tetrahedral sites and Ga^{3+} ions occupying octahedral sites. Zinc gallium oxide has a wide optical bandgap of about 4.4 eV, allowing tunability in the infrared (IR) to UV range and making it an ideal material for optoelectronic devices including FPDs, solar energy conversion devices, optical limiter for UV, and high-temperature stable gas sensors.[17] Moreover, undoped $ZnGa_2O_4$ gives a strong blue luminescence attributed to a transition via a self-activated center under UV or low-voltage electron excitation.

Here, the effects of doping Dy^{3+} in $ZnGa_2O_4$ are investigated.

Experimental

Dysprosium-doped $ZnGa_2O_4$ powder phosphors were prepared by mixing the starting materials, namely ZnO (99.99%, Alfa Aesar), Ga_2O_3 (99.99%, Alfa Aesar), and Dy_2O_3 (99.99%, Indian Rare Earths, Ltd.), stoichiometrically in ethanol medium followed by calcination at 1350°C for 12 h. The doping concentration of Dy^{3+} was varied in the range of 0.25–2.5 atom %. For comparison, $Zn_{1-x}Ga_2O_4:Dy_x$ ($x = 0$, 0.02, i.e., pure and 2 atom % doped sample where Dy^{3+} replaces Zn^{2+}) and $Ga_{2(1-x)}O_4:Dy_{2x}$ ($x = 0.02$, i.e., 2 atom % doped sample) phosphors were prepared. The crystal structure of the powder phosphors were analyzed using X-ray powder diffraction (XRD) method on a Rigaku diffractometer using Cu Kα radiation (1.5414 Å). The diffuse reflectance spectra (DRS) were recorded to analyze the bandgap using a Jasco V-570 spectrophotometer with an integrating sphere attachment. The reference used was $BaSO_4$. The room-temperature photoluminescent emission (PL) and excitation (PLE) spectra were recorded using Spex Fluoromax-3 Spectro-fluorimeter equipped with a 150 W xenon lamp as the excitation source.

Results and Discussion

The XRD patterns of $ZnGa_{2(1-x)}O_4:Dy_{2x}$ matched well with the standard reflections of host $ZnGa_2O_4$ for all dopant concentrations. No peaks of the used raw materials or other allotropic forms are detected. The absence of any secondary phase indicates that the samples have crystallized in the spinel structure similar to that of the host and that the dopant ions have been successfully dissolved into the host lattice. Figure 1 shows the XRD patterns of $ZnGa_{1.96}O_4:Dy_{0.04}$, $Zn_{0.98}Ga_2O_4:Dy_{0.02}$, and $Ga_{1.96}O_4:Dy_{0.04}$. Each of them closely resembles the respective host reflections. JCPDS data of the normal spinel $ZnGa_2O_4$ (card no. 38-1240) and monoclinic Ga_2O_3 (card no. 87-1901) is given for reference.

The DRS of the 2.5 atom % Dy^{3+}-doped sample is shown in Fig. 2. The bandgap of the sample was determined to be 4.45 eV from the $[(k/s)^*h\nu]^2$ vs $h\nu$ curves (inset of Fig. 2) obtained from diffuse reflectance measurements. The values of all the doped samples fall in the range 4.48 ± 0.05 eV for $ZnGa_{2(1-x)}O_4:Dy_{2x}$, which is close to the reported value of 4.55 eV for pure $ZnGa_2O_4$.[18]

* Electrochemical Society Student Member.
** E-mail: mkj@cusat.ac.in

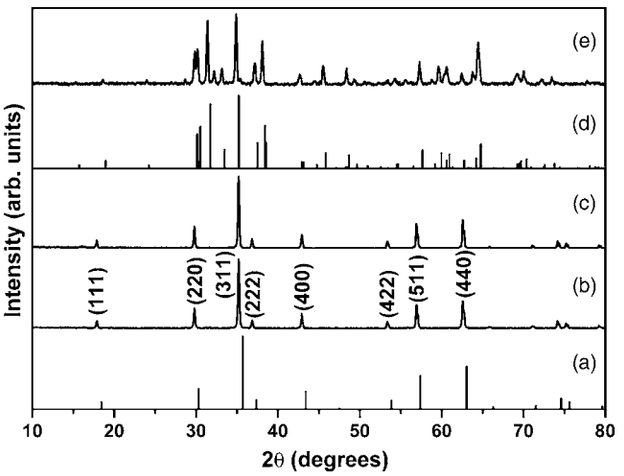

Figure 1. XRD patterns of JCPDS data of (a) $ZnGa_2O_4$, (b) $ZnGa_{1.96}O_4$:$Dy_{0.04}$, and (c) $Zn_{0.98}Ga_2O_4$:$Dy_{0.02}$ and JCPDS data of (d) Ga_2O_3, and (e) $Ga_{1.96}O_4$:$Dy_{0.04}$.

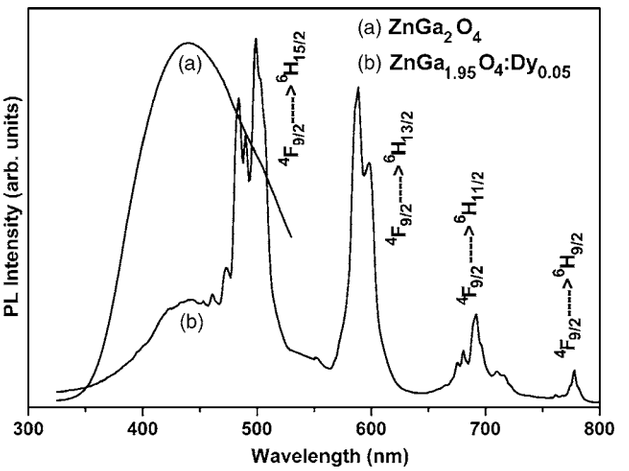

Figure 3. PL emission spectra of (a) pure $ZnGa_2O_4$ host and (b) 2.5 atom % Dy^{3+}-doped sample, λ_{exc} = 270 nm.

Figure 3 shows the PL emission spectra of pure $ZnGa_2O_4$ and 2.5 atom % Dy^{3+}-doped samples for an excitation wavelength of 270 nm. The undoped sample shows a strong broad blue luminescence with a peak at 439 nm resulting from the self-activated transition of regular O_h Ga–O groups.[19] The emission spectrum of the Dy^{3+}-doped sample exhibits both the emission band of the host extending from UV to blue and the characteristic fluorescence transitions $^4F_{9/2} \rightarrow {}^6H_J$ (J = 15/2, 13/2, 11/2, 9/2) of Dy^{3+} ions. There are four groups of characteristic lines in the dopant emission spectra: lines in the blue region (450–510 nm), lines in the yellow region (560–610 nm), and two groups of line spectra in the red region (660–720 nm and 755–800 nm) with their peak maxima at 499, 589, 692, and 778 nm, respectively. These emissions correspond to the spectral transitions $^4F_{9/2} \rightarrow {}^6H_{15/2}$, $^4F_{9/2} \rightarrow {}^6H_{13/2}$, $^4F_{9/2} \rightarrow {}^6H_{11/2}$, and $^4F_{9/2} \rightarrow {}^6H_{9/2}$, respectively, the dominant one being $^4F_{9/2} \rightarrow {}^6H_{15/2}$. The Stark levels of the multiplet manifolds could be well resolved as the crystal field had sufficient strength to lift off the degeneracy of the free-ion states of Dy^{3+} in the lattice.

The integral intensity of the blue emission ($^4F_{9/2}$–$^6H_{15/2}$) is stronger than that of the yellow emission ($^4F_{9/2}$–$^6H_{13/2}$). This spectral property of Dy^{3+} provides some information on the site occupation of Dy^{3+} in the host lattice. It is well known that the $^4F_{9/2}$ –$^6H_{13/2}$ yellow emission of Dy^{3+} is a hypersensitive transition that is strongly influenced by the crystal-field environment.[9,20,21] When Dy^{3+} is located at a low-symmetry local site (without an inversion symmetry), the yellow emission dominates the PL spectrum. The blue emission ($^4F_{9/2}$–$^6H_{13/2}$) is stronger than the yellow one when Dy^{3+} is located at a high-symmetry local site (with inversion symmetry). In the host lattice, Zn^{2+} ions occupy tetrahedral sites (T_d point symmetry without inversion center) coordinated by four oxygen atoms and Ga^{3+} ions occupy octahedral sites (O_h point symmetry with inversion-center) coordinated by six oxygen atoms. Because the blue emission dominates in the spectrum of all the samples, one can be sure that Dy^{3+} replaces Ga^{3+} more in the spinel-structured host. Moreover, the ionic radii of Dy^{3+} (0.0912 nm) is more compatible with Ga^{3+} (0.062 nm) for six coordination than that for four coordination. Though the ionic radii of Zn^{2+} is 0.074 nm for six coordination, Dy^{3+} ions rarely substitutes at its tetrahedral site due to charge imbalance.

The PLE spectrum (Fig. 4) of the Dy^{3+}-doped sample consists of a strong excitation band extending from 255 to 320 nm with peak maximum at 266 nm and a convolution of several weak lines (at

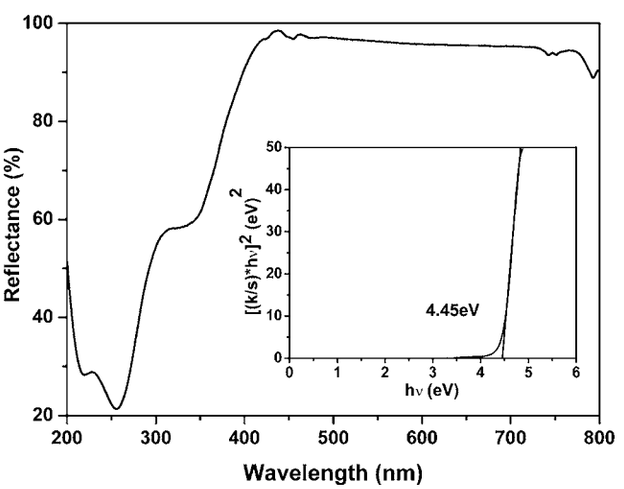

Figure 2. Diffuse reflectance spectra of $ZnGa_{1.95}O_4$:$Dy_{0.05}$ powder. (Inset) Plot of $[(k/s)h\nu]^2$ vs energy.

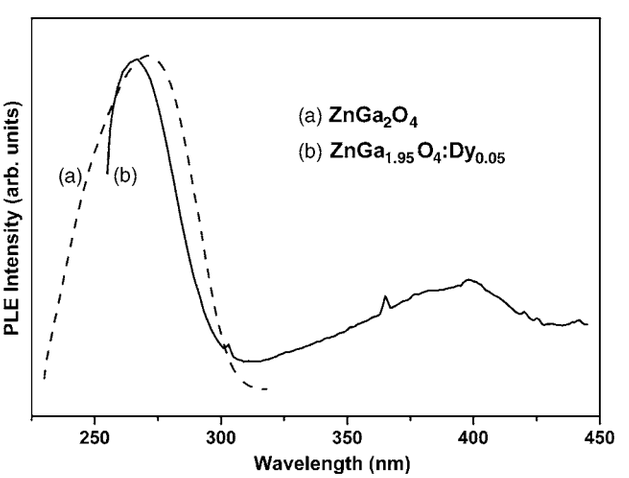

Figure 4. PLE spectra of (a) pure $ZnGa_2O_4$ host (λ_{em} = 439 nm) and (b) 2.5 atom % Dy^{3+}-doped sample (λ_{em} = 499 nm).

365, 399, 420, 425, and 442 nm) in the longer wavelength region. The weak lines positioned between 320 and 445 nm are due to the f-f transitions of Dy^{3+} within its $4f^9$ ground-state configuration.[9] The origin of the strong band can be correlated taking into consideration the excitation of the host. The excitation spectrum of pure $ZnGa_2O_4$ is also composed of a strong band ranging from 220 to 320 nm with a maximum at 271 nm whose spectral profile almost matches that of the doped sample. This indicates that the two strong excitation bands have the same origin, i.e., from the host lattice. The emission spectrum of undoped $ZnGa_2O_4$ contains a broad band ranging from 325 to 530 nm with peak maxima at 439 nm (blue emission) which is also present in the emission spectrum of the doped sample, but with reduced intensity. These results suggest that an energy transfer has occurred from the host lattice to the Dy^{3+} luminescence center. Here, this emission is not very efficient because a broad band of the host still persists with reduced intensity in the doped sample.

A luminescent material comprising of a sensitizer (S) and an activator (A) can exhibit either a radiative or a nonradiative energy transfer. Radiative transfer of energy is not very efficient in the case of intrashell transitions due to the low magnitude of the oscillator strength for absorption.[21] The transfer rate of the nonradiative resonance transfer mechanism depends both on the spectral overlap of the S emission band and the A absorption band and on the interaction between the initial and final states of the transfer between the S and the A. This interaction can be either an exchange interaction or an electric multipolar interaction; the transfer rate in either case depends on the distance R between the S and the A. The distance dependence is exponential for exchange interaction and R^{-n} dependence ($n = 6$ for dipole-dipole interactions and 8 for dipole-quadrupole interactions) for electric multipolar interactions. Thus, spectral overlap and distance R significantly affects energy-transfer rate.[21]

In the present case, there is only a small spectral overlap between $ZnGa_2O_4$ emission band (Ga being the sensitizer) and the $4f^9$ intraconfigurational absorption lines of Dy^{3+} (being the activator); the latter are forbidden by parity selection rule. Moreover, the strong absorption band of the activator lies outside the zinc gallate emission band. This makes the energy transfer by electric multipolar interactions less probable. Thus, the dominant energy-transfer mechanism in Dy^{3+}-activated $ZnGa_2O_4$ is most likely due to exchange interactions. This is more favored the smaller the value of R. For this, Dy^{3+} ions must replace Ga^{3+} at its octahedral site so that the energy of the strong emission band (peak at 439 nm) resulting from the transition of regular O_h Ga–O groups can be efficiently and effectively transferred to the luminescent center Dy^{3+} by nonradiative resonance mechanism mediated by exchange interactions.

A comparison was made between the PL emission spectra of host $ZnGa_2O_4$ along with the emission spectra of $Zn_{1-x}Ga_2O_4:Dy_x$, $ZnGa_{2(1-x)}O_4:Dy_{2x}$, and $Ga_{2(1-x)}O_4:Dy_{2x}$ prepared under similar synthetic conditions for a doping concentration of 2 atom % (Fig. 5). The emission spectra of $Zn_{0.98}Ga_2O_4:Dy_{0.02}$ exhibits the UV-to-blue-emission band of the host itself, whereas that of $ZnGa_{1.96}O_4:Dy_{0.04}$ includes both the emission band of $ZnGa_2O_4$ and the characteristic fluorescence transitions $^4F_{9/2}-{}^6H_J$ of the dopant. The blue emission of the $Zn_{0.98}Ga_2O_4:Dy_{0.02}$ sample is more intense than the host. But the $ZnGa_{1.96}O_4:Dy_{0.04}$ compound gives weaker $ZnGa_2O_4$ emission and strong dysprosium emissions. In the former case, because Dy^{3+} is thought to substitute for Zn^{2+} at its tetrahedral site, the energy transfer via exchange interactions is greatly reduced due to larger *S-A* distance (R) suppressing Dy^{3+} emissions. In the latter case, Dy^{3+} emission gets enhanced as R is greatly reduced. The PL emission intensity of $Ga_{1.96}O_4:Dy_{0.04}$ is much stronger than $ZnGa_{2(1-x)}O_4:Dy_{2x}$, indicating that host sensitization is more effective in the former.

Figure 6 compares the PL emission spectra of the $ZnGa_{2(1-x)}O_4:Dy_{2x}$ samples with different doping concentrations, all spectra recorded at an excitation wavelength of 270 nm. In the low-

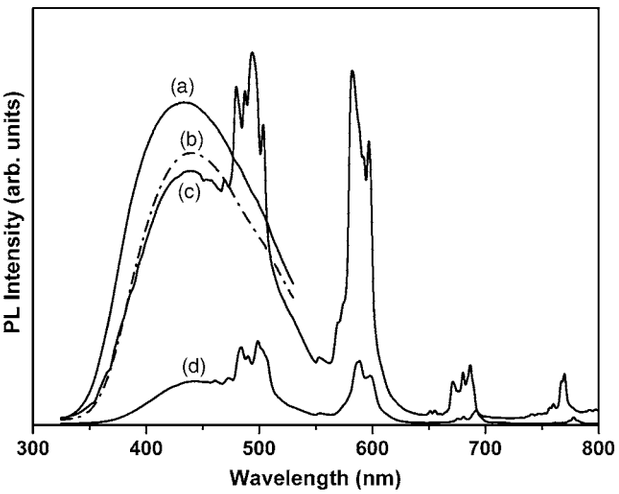

Figure 5. PL emission spectra of (a) $Zn_{0.98}Ga_2O_4:Dy_{0.02}$, (b) pure $ZnGa_2O_4$ and (c) $Ga_{1.96}O_4:Dy_{0.04}$, and (d) $ZnGa_{1.96}O_4:Dy_{0.04}$, $\lambda_{exc} = 270$ nm.

dopant-concentration range ($x = 0.0025$ to 0.01), intensive blue-emission band of the host and weaker luminescent transitions of Dy^{3+} activator are observed. The emission maximum occurs for the 1 atom % doped sample, and hereafter it weakens and red-shifts gradually due to larger Zn/Ga ratio.[22,23] In the dopant-concentration range ($x = 0.0125$–0.025), the characteristic luminescent transitions of Dy^{3+} activator predominates over the host emission and the intensity ratio I_{499}/I_{589} (I_{499} and I_{589} correspond to the maxima of $^4F_{9/2} \rightarrow {}^6H_{15/2}$ and $^4F_{9/2} \rightarrow {}^6H_{13/2}$ fluorescent transitions of Dy^{3+}) is such that a luminescent emission that appears white to the human eye is observed. The variation of the host and the activator emissions with doping concentration is shown in the inset of Fig. 6. It is quite evident that the host emission intensity falls below the activator emission intensity for all dopant concentrations above 1 atom %, indicative of host-sensitized luminescence.

For some suitable blue-to-yellow intensity ratio I_{499}/I_{589}, Dy^{3+} emits white light. The intensity ratio I_{499}/I_{589} plotted in Fig. 7 reveals that when the ratio falls in between 1 and 1.5, the samples exhibit white luminescence, and this has been observed in the case of all Dy^{3+}-doped samples for dopant concentration above

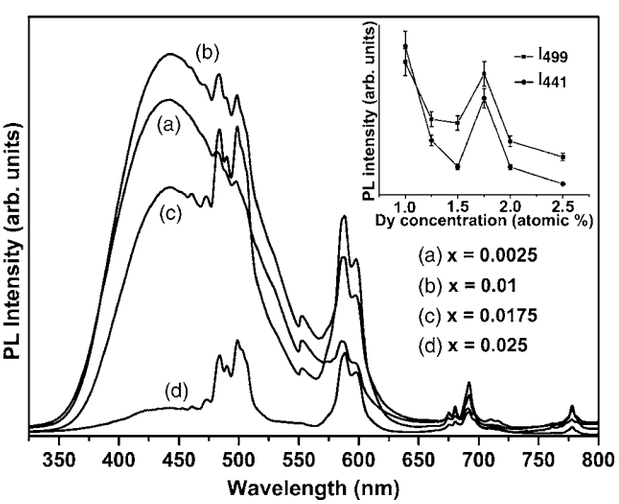

Figure 6. PL emission spectra of $ZnGa_{2(1-x)}O_4:Dy_{2x}$ ($x = 0.0025$, 0.01, 0.0175, 0.025), $\lambda_{exc} = 270$ nm. (Inset) Variation in the PL intensity I_{499} (activator) and I_{441} (host) with dopant concentration.

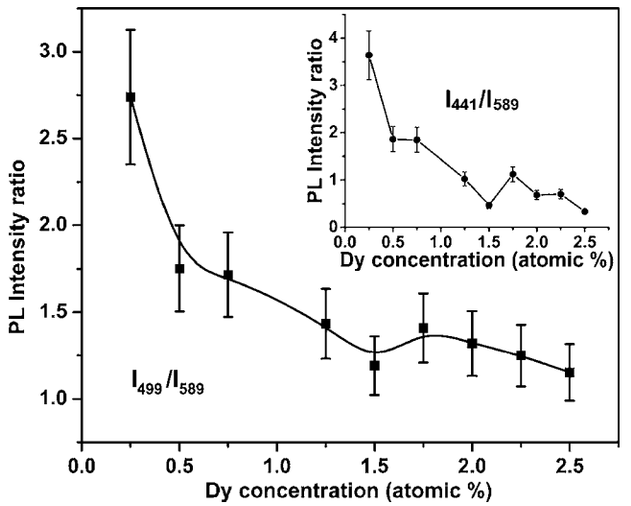

Figure 7. Variation in the PL intensity ratios I_{499}/I_{589} and I_{441}/I_{589} (inset) with dopant concentration.

1 atom %. This observation also supports the fact that Dy^{3+} substitutes the element with the same valency[7] in the host. The inset shows that the intensity ratio I_{441}/I_{589} (I_{441} corresponds to the host blue PL intensity at 441 nm) falls below 1 for all samples above $x = 0.01$, i.e., the whiteness is due to the simultaneous blue and yellow emissions of Dy^{3+} itself. Both the intensity ratios lie above 1.5 for low dopant concentrations ($x = 0.0025$–0.01) and these samples are found to exhibit bluish luminescence. The blue-to-yellow intensity ratio I_{494}/I_{582} of $Ga_{1.96}O_4$:$Dy_{0.04}$, which also gave white luminescence, was found to be 1.05.

The PL emissions of the samples were gauged employing the CIE coordinates (Fig. 8). The CIE coordinates of the Dy^{3+}-doped samples lie in between that of the $ZnGa_2O_4$ host ($x = 0.13$, $y = 0.16$) and that for achromatic white ($x = 0.33$, $y = 0.33$). The

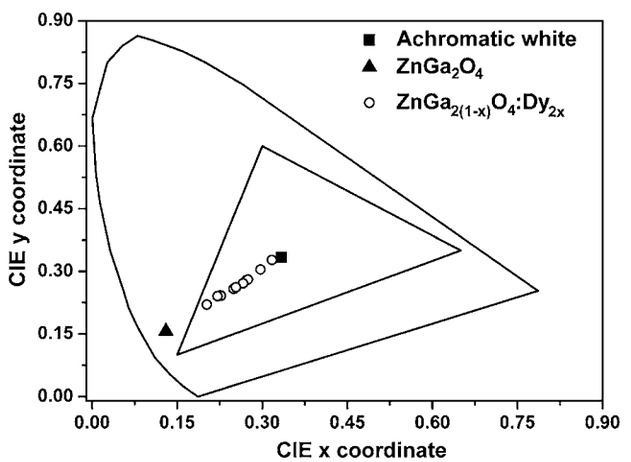

Figure 8. CIE chromaticity diagram of the $ZnGa_{2(1-x)}O_4$:Dy_{2x} ($0.0025 \leq x \leq 0.025$); CIE coordinates of $ZnGa_2O_4$ host and achromatic white are shown for comparison.

2.5 atom % Dy^{3+}-doped sample shows the best white emission; its CIE coordinates were calculated to be $x = 0.32$ and $y = 0.33$ and it lies just to the left of achromatic white in the chromaticity diagram.[24,25] The $Ga_{1.96}O_3$:$Dy_{0.04}$ sample prepared for comparison also gave a white emission and has a higher intensity than the Dy^{3+}-doped $ZnGa_2O_4$ sample, but the CIE coordinates were calculated to be $x = 0.27$, $y = 0.27$. That is, the white emission of $Ga_{1.96}O_3$:$Dy_{0.04}$ phosphor is much inferior to that of $ZnGa_{1.95}O_4$:$Dy_{0.05}$ phosphor.

Conclusion

$ZnGa_{2(1-x)}O_4$:Dy_{2x} phosphors were prepared by conventional solid-state reaction technique. The doped samples exhibit the normal spinel-phase development as the host. PL studies reveal the fact that Dy^{3+} ions replace Ga^{3+} ions in the host lattice at their octahedral sites. The source of the white emission in the doped samples is the nonradiative resonant energy transfer via exchange interaction between the host and the activator. The poor spectral overlap accounts for the reduced PL emission intensity of the doped samples. The best white emission is obtained for the sample with a dopant concentration of 2.5 atom % whose CIE coordinates are found to be $(x,y) = (0.32,0.33)$. The present investigation highlights the possibility of Dy^{3+}-doped $ZnGa_2O_4$ as an active layer in alternating current thin film electroluminescent (ACTFEL) devices.

Acknowledgments

The authors thank the government of India for financial support. K.M.K. thanks CSIR for the grant of a fellowship.

References

1. J. S. Kim, J. Y. Kang, P. E. Jeon, J. C. Choi, H. L. Park, and T. W. Kim, *Jpn. J. Appl. Phys., Part 1*, **43**, 989 (2004).
2. J. K. Park, M. A. Lim, C. H. Kim, H. D. Park, J. T. Park, and S. Y. Choi, *Appl. Phys. Lett.*, **82**, 683 (2003).
3. N. Lakshminarasimhan and U. V. Varadaraja, *J. Electrochem. Soc.*, **152**, H152 (2005).
4. J. S. Kim, P. E. Jeon, J. C. Choi, H. L. Park, S. I. Mho, and G. C. Kim, *Appl. Phys. Lett.*, **84**, 2931 (2004).
5. J. B. Gruber, B. Zandi, U. V. Valiev, and S. A. Rakhimov, *J. Appl. Phys.*, **94**, 1030 (2003).
6. B. Liu, C. Shi, and Z. Qi, *Appl. Phys. Lett.*, **86**, 191111 (2005).
7. Q. Su, Z. Pei, L. Chi, H. Zhang, Z. Zhang, and F. Zou, *J. Alloys Compd.*, **192**, 25 (1993).
8. Q. Su, Z. Pei, J. Lin, and F. Xue, *J. Alloys Compd.*, **225**, 103 (1995).
9. W. Y. Shen, M. L. Pang, J. Lin, and J. Fang, *J. Electrochem. Soc.*, **152**, H25 (2005).
10. X. Liu, C. Lin, Y. Luo, and J. Lin, *J. Electrochem. Soc.*, **154**, J21 (2007).
11. J. Lin and Q. Su, *J. Alloys Compd.*, **210**, 159 (1994).
12. J. S. Kim, S. G. Lee, H. L. Park, J. Y. Park, and S. D. Han, *Mater. Lett.*, **58**, 1354 (2004).
13. T. Minami, Y. Kuroi, and S. Takata, *J. Vac. Sci. Technol. A*, **14**, 1736 (1996).
14. T. Minami, T. Maeno, Y. Kuroi, and S. Takata, *Jpn. J. Appl. Phys., Part 2*, **34**, L684 (1995).
15. T. K. Tran, W. Park, J. W. Tomm, B. K. Wagner, S. M. Jacobsen, C. J. Summers, P. N. Yocom, and S. K. McClelland, *J. Appl. Phys.*, **78**, 5691 (1995).
16. L. E. Shea, R. K. Datta, and J. J. Brown, Jr. *J. Electrochem. Soc.*, **141**, 2198 (1994).
17. L. Satyanarayana, C. V. Gopal Reddy, S. V. Manoram, and V. J. Rao, *Sens. Actuators B*, **46**, 1 (1998).
18. R. Reshmi, K. Mini Krishna, R. Manoj, and M. K. Jayaraj, *Surf. Coat. Technol.*, **198**, 345 (2005).
19. I. K. Jeong, H. L. Park, and S. Mho, *Solid State Commun.*, **105**, 179 (1998).
20. M. L. Pang, W. Y. Shen, and J. Lin, *J. Appl. Phys.*, **97**, 033511 (2005).
21. Z. Xu, Y. Li, Z. Liu, and D. Wang, *J. Alloys Compd.*, **391**, 202 (2005).
22. M. Yu, J. Lin, Y. H. Zhou, and S. B. Wang, *Mater. Lett.*, **56**, 1007 (2002).
23. J. W. Moon, H. S. Moon, E. S. Oh, H. I. Kang, J. S. Kim, H. L. Park, and T. W. Kim, *Int. J. Inorg. Mater.*, **3**, 575 (2001).
24. J. S. Kim, J. S. Kim, T. W. Kim, H. L. Park, Y. G. Kim, S. K. Chang, and S. D. Han, *Solid State Commun.*, **131**, 493 (2004).
25. W. N. Kim, H. L. Park, and G. C. Kim, *Mater. Lett.*, **59**, 2433 (2005).